BJP British Journal of Pharmacology

DOI:10.1111/bph.13082
www.brjpharmacol.org

RESEARCH PAPER

The orally active urotensin receptor antagonist, KR36676, attenuates cellular and cardiac hypertrophy

K S Oh[1,2,*], J H Lee[1,*], K Y Yi[2,3], C J Lim[2,3], S Lee[4], C H Park[1], H W Seo[1] and B H Lee[1,5]

[1]*Research Center for Drug Discovery Technology, Korea Research Institute of Chemical Technology, Daejeon, Korea,* [2]*Department of Medicinal and Pharmaceutical Chemistry, University of Science and Technology, Daejeon, Korea,* [3]*Research Center for Medicinal Chemistry, Korea Research Institute of Chemical Technology, Daejeon, Korea,* [4]*Department of Biomedical Technology, College of Engineering, Sangmyung University, Cheonan, Korea, and* [5]*Graduate School of New Drug Discovery and Development, Chungnam National University, Daejeon, Korea*

Correspondence
Byung Ho Lee, Research Center for Drug Discovery Technology, Korea Research Institute of Chemical Technology, Daejeon, Korea. E-mail: bhlee@krict.re.kr

*These two authors contributed equally to this work.

Received
4 November 2014
Revised
11 December 2014
Accepted
13 January 2015

BACKGROUND AND PURPOSE

Blockade of the actions of urotensin-II (U-II) mediated by the urotensin (UT) receptor should improve cardiac function and prevent cardiac remodelling in cardiovascular disease. Here, we have evaluated the pharmacological properties of the recently identified UT receptor antagonist, 2-(6,7-dichloro-3-oxo-2H-benzo[b][1,4]oxazin-4(3H)-yl)-N-methyl-N-(2-(pyrrolidin-1-yl)-1-(4-(thiophen-3-yl)phenyl) ethyl)acetamide (KR36676).

EXPERIMENTAL APPROACH

Pharmacological properties of KR36676 were studied in a range of *in vitro* assays (receptor binding, calcium mobilization, stress fibre formation, cellular hypertrophy) and *in vivo* animal models such as cardiac hypertrophy induced by transverse aortic constriction (TAC) or myocardial infarction (MI).

KEY RESULTS

KR36676 displayed high binding affinity for the UT receptor (K_i: 0.7 nM), similar to that of U-II (0.4 nM), and was a potent antagonist at that receptor (IC_{50}: 4.0 nM). U-II-induced stress fibre formation and cellular hypertrophy were significantly inhibited with low concentrations of KR36676 (≥0.01 μM). Oral administration of KR36676 (30 mg·kg^{-1}) in a TAC model in mice attenuated cardiac hypertrophy and myocardial fibrosis. Moreover, KR36676 restored cardiac function and myocyte size in rats with MI-induced cardiac hypertrophy.

CONCLUSIONS AND IMPLICATIONS

A highly potent UT receptor antagonist exerted anti-hypertrophic effects not only in infarcted rat hearts but also in pressure-overloaded mouse hearts. KR36676 could be a valuable pharmacological tool in elucidating the complicated physiological role of U-II and UT receptors in cardiac hypertrophy.

Abbreviations

$H9c2_{UT}$, H9c2 cells stably expressing human urotensin-II receptor; KR36676, 2-(6,7-dichloro-3-oxo-2H-benzo[b][1,4]oxazin-4(3H)-yl)-N-methyl-N-(2-(pyrrolidin-1-yl)-1-(4-(thiophen-3-yl)phenyl) ethyl)acetamide; LV, left ventricular; SB657510, 2-bromo-*N*-[4-chloro-3-[[(3*R*)-1-methylpyrrolidin-3-yl]oxy] phenyl]-4,5-dimethoxybenzenesulfonamide, HCl); SD, Sprague-Dawley; U-II, urotensin-II; UT, urotensin

Tables of Links

TARGETS
GPCR[a]
UT receptor, GPR14
Enzymes[b]
ERK1/2
JNK
p38

LIGANDS
Captopril
SB611812
U-II, urotensin II
Urantide

These Tables list key protein targets and ligands in this article which are hyperlinked to corresponding entries in http://www.guidetopharmacology.org, the common portal for data from the IUPHAR/BPS Guide to PHARMACOLOGY (Pawson *et al.*, 2014) and are permanently archived in the Concise Guideto PHARMACOLOGY 2013/14 ([a,b]Alexander *et al.*, 2013a,b).

Introduction

Urotensin-II (U-II) is a neuropeptide and endogenous ligand of the GPCR first known as the orphan GPR14 and now as the urotensin (UT) receptor (Ames *et al.*, 1999). U-II is the most potent endogenous vasoconstrictor currently known (Douglas and Ohlstein, 2000). In normal myocardium, the expression of UT receptors is low or undetectable. However, plasma U-II concentrations as well as tissue expression levels of U-II and UT receptors are up-regulated in various cardiovascular diseases including myocardial infarction (MI), pulmonary hypertension and heart failure (Bousette and Giaid, 2006; Ross *et al.*, 2010). Thus, the UT system is considered a promising pharmacological target in such conditions and, accordingly, a number of UT receptor antagonists have been developed (Tsoukas *et al.*, 2011).

Cardiac hypertrophy is an adaptive response to pressure overload that aims to maintain cardiac function. However, persistent stresses (i.e. chronic pressure overload) cause it to become a maladaptive response, leading to complications, such as inflammation, fibrosis and ventricular hypertrophy, which ultimately can contribute to cardiac dysfunction, and subsequent heart failure (McKinsey and Olson, 2005; Heineke and Molkentin, 2006). Recent studies have shown that the UT system is critically involved in the pathology of cardiac hypertrophy. U-II-mediated hypertrophy has been found in rat neonatal cardiomyocytes and the H9c2 rat cardiomyoblast cell line expresses high levels of UT receptor (Tzanidis *et al.*, 2003; Johns *et al.*, 2004; Onan *et al.*, 2004). Furthermore, an infusion of U-II into rats potentiated isoprenaline-induced fibrosis and cardiac hypertrophy (Zhang *et al.*, 2007). Several mechanisms underlying the U-II and UT receptor-mediated cardiac hypertrophy have been suggested, including up-regulation of inflammatory cytokines and reactive oxygen species (Johns *et al.*, 2004; Liu *et al.*, 2009), and activation of signalling pathways such as $G\alpha_q$- and Ras-dependent, MAPKs, and the Akt/GSK-3β signalling pathways (Tzanidis *et al.*, 2003; Onan *et al.*, 2004; Gruson *et al.*, 2010). Most recently, a deleterious elevation of the UT system has been found in the metabolic syndrome, which is a critical risk factor for cardiovascular diseases (Barrette and Schwertani, 2012; You *et al.*, 2012; Li *et al.*, 2014). These results raise the possibility that U-II and UT receptors are involved in the pathogenesis of cardiac remodelling.

There were several experimental studies of the effects of UT receptor antagonists in cardiac hypertrophy. Peptidic UT receptor antagonists, BIM-23127 (Johns *et al.*, 2004) and urantide (Gruson *et al.*, 2010), inhibited U-II-induced hypertrophy in cardiomyocytes. In a rat model of coronary artery ligation, the non-peptide UT receptor antagonist, SB611812, attenuated cardiac dysfunction while reducing heart weight (HW; Bousette *et al.*, 2006). However, the anti-hypertrophic effects of urantide and SB657510 (2-bromo-*N*-[4-chloro-3-[[(3*R*)-1-methylpyrrolidin-3-yl]oxy] phenyl]-4,5-dimethoxybenzenesulfonamide, HCl)), another non-peptide UT receptor antagonist, was absent in hearts with pressure overloaded by aortic constriction (Kompa *et al.*, 2010; Esposito *et al.*, 2011). Thus, the effects of UT receptor antagonism on cardiac hypertrophy in pathological conditions are still not clear and require additional study for clarification. Hence, the identification of UT receptor antagonists with high potency and selectivity is an important requirement in order to define the role of the UT system in cardiac hypertrophy.

In the search for effective UT receptor antagonists, we recently identified 2-(6,7-dichloro-3-oxo-2H-benzo[b][1,4] oxazin-4(3H)-yl)-N-methyl-N-(2-(pyrrolidin-1-yl)-1-(4-(thiophen-3-yl)phenyl) ethyl)acetamide (KR36676) as a novel and potent UT receptor antagonist. The present study aimed to detail the pharmacological characteristics of KR36676 by investigating (i) its UT receptor affinity, selectivity and antagonistic activity, (ii) the beneficial inhibitory effects on U-II-mediated cellular events such as stress fibre formation and cellular hypertrophy, (iii) the *in vivo* efficacy on U-II-induced ear flushing, and (iv) the anti-hypertrophic activity and cardiac function in the mouse model of pressure-overload hypertrophy and the rat model of MI-induced cardiac hypertrophy.

Methods

Animals

All animal care and experimental procedures were reviewed and approved by the Institutional Animal Care and Use Committee of the Korea Research Institute of Chemical Technology (KRICT). All studies involving animals are reported in accordance with the ARRIVE guidelines for reporting experi-

ments involving animals (Kilkenny *et al.*, 2010; McGrath *et al.*, 2010). A total of 198 animals were used in the experiments described here. Male C57BL/6 mice and Sprague-Dawley (SD) rats were purchased from Orient Bio Inc. (Sungnam, Gyeonggi, Korea). Animals were conditioned for 1 week at 22.0 ± 2°C with a constant humidity of 55 ± 5%, a cycle of 12 h light/dark, and free access to food and tap water.

Cell culture

For the cellular functional assay, aequorin parental cells were grown in Eagle's minimum essential medium supplemented with 10% FBS, penicillin (100 IU·mL^{-1}), streptomycin (100 μg·mL^{-1}) and zeocin (10 μg·mL^{-1}). To establish a stable aequorin cell line for the human UT (hUT) receptor, the cDNA for the this receptor (UTR2/GPR14, GenBank Acc# NM_018949 except C51T) in pcDNA 3.1+ was transfected to the aequorin parental cell line (HEK293-aeq, ES-000-A30) with Lipofectamine 2000. During the clonal selection for the search of maximum calcium responses by U-II in transfected cells, the concentration of G418 was kept at 400 mg·mL^{-1}. Cells were discarded after 2–3 months of continuous growth with splitting, and new cells were prepared from a frozen stock to maintain the stability of agonist signals.

For the cell-based phenotype assay, rat heart-derived H9c2 cells (ATCC, Rockville, MD, USA) were maintained at 1 × 10^6 cells·mL^{-1} in DMEM supplemented with 10% FBS, L-glutamine (2 mM) and antibiotics. Stable cells expressing the hUT receptor were obtained by transfection of cDNA into H9c2 cells. In a cell-based phenotype assay, cells were starved in serum-free media for 24 h and then stimulated with 0.1 μM U-II in the presence of KR36676 or SB657510 for the indicated periods. The maximum concentration of stock solution (dimethyl sulfoxide) in experimental media was kept at 0.1%. Cells were cultured in 16-well chamber slides (for immunofluorescent staining) or in 6-well plates (for cellular hypertrophy).

Radioligand receptor binding assay for hUT receptors

The UT binding affinity was determined by radio-ligand binding assay in Eurofins Panlabs (Test No.: AB22313; Taipei, Taiwan). Briefly, to evaluate K_i values of investigating ligands, a hUT receptor binding assay was performed with 0.1 nM [^{125}I] U-II for 2 h at 37°C in 20 mM Tris-HCl, pH 7.4, supplemented with 5 mM $MgCl_2$, and 0.5% bovine serum albumin. The human recombinant UT receptor membrane was used (UT/CHO-K1 membrane). K_D values of ligand and B_{max} of receptor were 0.2 nM and 0.42 pmol·mg^{-1} respectively. Non-specific binding was defined in the presence of 1 μM U-II. Ligand binding was determined by filtration of the assay mixture over GF/C Whatman filters. After washing the filters, liquid scintillation counting was used to quantify radioactivity.

Cell-based functional assay for hUT receptor activity

A functional assay based on the luminescence of mitochondrial aequorin. Cells collected from the culture plates were resuspended (1 × 10^6 cells·mL^{-1}) in the assay buffer (DMEM/HAM's F12 without phenol red, with L-glutamine, 15 mM HEPES, pH 7.0 and 0.1% BSA). Then, the cells were incubated overnight at room temperature in the dark with 5 μM of coelenterazine with constant agitation. After loading the coelenterazine, the cells were diluted with assay buffer (1 × 10^5 cells·mL^{-1}) and incubated for 60 min. To measure antagonist activity, cells were treated with KR36676 or SB657510 at the indicated dilutions and incubated for 15 min. Then, 50 μL of U-II (0.1 μM) was added and the light emission was recorded to determine cell activation using a Mithras LB 940 Multilabel Reader (Berthold Technologies, Bad Wildbad, Germany) and results were expressed in relative luminescence units.

Immunofluorescent staining for F-actin stress fibre formation

For immunofluorescent staining, H9c2$_{UT}$ cells were plated on a 16-well chamber slide (Thermo Fisher Scientific, Rochester, NY, USA) at a density of 5 × 10^3 cells·mL^{-1}. After pre-incubation with KR36676 or SB657510 (0.001–0.1 μM) for 2 h, the cells were treated with U-II (0.1 μM) for 2 h, fixed with 4% paraformaldehyde for 20 min, incubated with 0.5% Triton X-100 for 10 min, and then blocked with 1% BSA for 30 min. Cells were then probed with Alexa Fluor 586 Phalloidin (Invitrogen, Carlsbad, CA, USA; diluted 1:1000) for 30 min at room temperature in the dark, washed with PBS, and stained with Hoechst 33342. The fluorescent images were examined with a fluorescence microscope at a magnification of 400× (Nikon, Tokyo, Japan).

Measurement of cellular hypertrophy

For measurement of cellular hypertrophy, H9c2$_{UT}$ cells were seeded at a density of 5 × 10^3 cells·mL^{-1} on an 8-well chamber slide (Thermo Fisher Scientific). After 2 days, the cells were maintained in serum-free medium overnight. After pretreatment with KR36676 or SB657510 (0.001–0.1 μM) for 2 h, cells were treated with U-II (0.1 μM) in serum-free medium with a fresh supply of KR36676 or SB657510 for 24 h to induce a hypertrophic response. After inducing cellular hypertrophy, adherent cells were fixed with 1% glutaraldehyde for 30 min and stained with 0.1% Crystal Violet dye for 1 h. Four random photographs were taken from each sample, and at least 140 individual cells were examined in each group. Cell size was analysed using Image-Pro PLUS software (Media Cybernetics, Silver Spring, MD, USA).

Measurement of U-II-induced ear flushing

The U-II-induced ear flushing model accompanied by increase of ear temperature has been used to determine whether a UT receptor antagonist could block an U-II-mediated effect *in vivo* (Qi *et al.*, 2007). Briefly, SD rats (380–420 g) were acclimatized to 22 ± 0.5°C for at least 2 h before the experiment. The ear pinna temperature was measured using a non-contact infrared thermometer (Optris LaserSight, Optirs GmbH, Germany) in conscious animals. After measurement of baseline temperature, each group received either an i.p. injection of KR36676 (1, 3 or 10 mg·kg^{-1}), SB657510 (3, 10 or 30 mg·kg^{-1}) or vehicle (polyethylene glycol 400) at 5 min prior to U-II injection. To further test oral efficacy, KR36676, SB657510 or vehicle (0.5% carboxymethyl cellulose) was orally administered 30 min prior to U-II injec-

tion. U-II (10 nmol·kg^{-1}·mL^{-1}) was injected s.c. in the mid-scapular region (0 min time point). The ear pinna temperature was subsequently measured at every 3 min for a period of up to 45 min.

Transverse aortic constriction (TAC) in mice

The TAC model was performed to induce pressure-overload hypertrophy as described previously (deAlmeida *et al.*, 2010). Briefly, male C57BL/6 mice (20–24 g) were anaesthetized with an i.p. injection of Zoletil (30 mg·kg^{-1}) and Rompun (10 mg·kg^{-1}). Body temperature was maintained at 37°C with a heating pad. Mice were orally intubated and ventilated with room air using a small animal ventilator (SAR-830/P; CWE, Inc., Ardmore, PA, USA). After midline sternotomy, the transverse aortic arch between the innominate and left common carotid artery was ligated with a 26-gauge needle using 6-0 silk suture, and then the needle was quickly removed. Mice were allowed to recover from surgery in a warm incubator until fully awake. Sham-operated mice were subjected to the same surgical procedure without constricting the aorta. The first dose of KR36676 (10 or 30 mg·kg^{-1}), captopril (30 mg·kg^{-1}; Sigma-Aldrich) or vehicle (0.5% carboxymethyl cellulose) was given by oral gavage 1 h prior to surgery. Then, all treatments were administered once a day for 2 weeks following surgery. The dosage of KR36676 was chosen based on the results of the ear flushing study. Captopril, an ACE inhibitor, was used to compare the *in vivo* effects of KR36676. At 2 weeks after TAC, left ventricular (LV) haemodynamics was assessed under anaesthesia (Zoletil/Rompun). The right carotid artery was cannulated with a 1.0 F Mikro-Tip pressure transducer (SPR-1000; Millar Instruments, Houston, TX, USA). After advancing the catheter into the LV cavity, the heart rate and LV systolic pressure (LVSP) were recorded using the MPVS-400 system (Millar Instruments). At the end of the haemodynamic measurements, the hearts were dissected and weighed to determined cardiac hypertrophy.

MI in rats

The left anterior descending coronary artery (LAD) was occluded as described previously (Oh *et al.*, 2009). Male SD rats (260–300 g) were anaesthetized with sodium pentobarbital (60 mg·kg^{-1}, i.p.) and ventilated with room air. After left thoracotomy, LAD artery was either ligated or left untied using 5-0 silk suture. The rats were classified into three groups: sham, MI + vehicle and MI + KR36676 (30 mg·kg^{-1}, p.o.). At 4 weeks after MI, cardiac function was assessed. The right carotid artery was cannulated with a 2F micro-tip pressure-volume catheter transducer (SPR-838; Millar Instruments). After advancing the catheter into the LV cavity, LVSP, end-diastolic pressure and heart rate were recorded. The rates of maximum positive and negative LV pressure development (+dP/dt$_{max}$ and –dP/dt$_{max}$) were also examined. To determine stroke volume, cardiac output and stroke work, a pressure–volume loop was generated by simultaneously recording the LV pressure and volume in the working heart. Data were analysed with Millar's PVAN software (version 3.3).

Histology and immunohistochemistry

After measuring heart weight , the left ventricles with the septum were fixed with 10% formalin and embedded in paraffin. The transverse sections (5 μm) were stained with hematoxylin and eosin for overall morphology, and Picrosirius Red (ScyTek Laboratories, Logan, UT, USA) and Masson's trichrome (Diagnostic BioSystems, Pleasanton, CA, USA) for detection of fibrosis. At least 150 cells per heart were measured to determine the average of myocyte cross-sectional area. The interstitial fibrosis was determined by measuring Picrosirius Red-stained area in 10 random, non-overlapped microscopic fields (magnification ×200) per tissue from the mid ventricle to the endocardium excluding perivascular areas, and expressed as percentage of fibrous tissue areas in the entire visual fields. After Masson's trichrome staining, the perivascular fibrosis was determined as the ratio of the area of collagen fibres surrounding the vessel to the area of vascular wall. The infarct size was calculated from Masson's trichrome-stained rat hearts as the percentage of total infarcted epicardial and endocardial lengths to total LV circumferences (Fishbein *et al.*, 1978). The expansion index was calculated with the formula: expansion index = (LV cavity area/total LV area) × (septal thickness/scar thickness; Alhaddad *et al.*, 1995). Additional rat heart sections were immunostained to evaluate the expression of U-II and UT receptors in the peri-infarct zone. The sections were incubated with primary antibodies (Alpha Diagnostic International, San Antonio, TX, USA): anti-rat U-II IgG (1:1000) or GPR14 IgG (1:100), followed by incubation with secondary antibodies. The sections were then incubated with ABC solution (Vector Laboratories, Burlingame, CA, USA) and developed using the diaminobenzidine substrate with haematoxylin counterstain. The images of the infarct border zone were captured and examined.

Western blot

Equal amounts of protein (30 μg) from LV tissues were loaded in SDS-PAGE and transferred to nitrocellulose membranes. After blocking, membranes were incubated overnight with primary antibodies (Cell Signaling Technology, Beverly, MA, USA; 1:1000) against total or phosphorylated form of ERK1/2, p38 and JNK. After incubation with HRP-conjugated secondary antibodies, immunoreactive bands were detected by the LumiGLO kit (New England Biolabs, Ipswich, MA, USA). Values for phosphorylated ERK1/2, p38, and JNK protein were normalized to the total ERK1/2, p38 and JNK protein respectively.

Measurement of receptor selectivity

The receptor selectivity of KR36676 at the concentration of 10 or 1 μM were determined by Safety Screen panel services in Eurofins Panlabs (Test No.: AB22557, AB22314) using radioligand binding assays for 86 distinct mammalian receptors, ion channels, transporter such as the adenosine $A_{1,}$ A_{2A} receptor$_s$; $\alpha_{1A,\ 1B,\ 1D,\ 2A,\ 2B}$; $\beta_{1,\ 2}$ adrenoceptors; androgen; angiotensin AT_1; bradykinin B_2; N, L-type calcium channel; cannabinoid $CB_{1,\ 2}$; chemokine $CCR_{1,\ 2}$ receptors; cholecystokinin $CCK_{1,\ 2}$ receptors; dopamine $D_{1,\ 2L,\ 2s}$ receptors; endothelin ET_A; oestrogen ERα; $GABA_{A,\ B1A}$ receptor; glucocorticoid; glutamate AMPA, kainate, $mGlu_5$; glycine; NMDA receptor; histamine $H_{1,\ 2}$; LT T_1, melanocortin $MC_{1,\ 4}$; muscarinic $M_{1,\ 2,\ 3,\ 4;}$ neuropeptide Y_1; nicotinic ACh; nicotinic ACh α_1; opioid δ_1, κ, μ; platelet activating factor; ATP-sensitive potassium channel;

PPARγ; progesterone PR-B; serotonin 5-$HT_{1A, 1B, 2A, 2B, 2C, 3}$; sodium channel site 2; tachykinin NK_1; adenosine transporter; dopamine transporter; GABA transporter; noradrenaline transporter; 5-HT) transporter; vasopressin V_{1A} receptors and several enzymes including ATPase; cholinesterase; COX-1, -2; MAO-A, MAO-B; ACE; CTSG peptidase; PDE3, 4; non-selective PKC; insulin receptor kinase; protein TK LCK.

Pharmacokinetic study

The plasma concentration of KR36676 was measured in SD rats (260–300 g) following intravenous or oral administration at 10 mg·kg^{-1}. The plasma was collected at 0.03, 0.08, 0.17, 0.33, 0.5, 1, 2, 4, 6, 8 and 24 h after dosing, and the plasma levels of KR36676 were measured using HPLC.

Data analysis

All values were expressed as mean ± SEM. Concentration-response curves were analysed by non-linear regression using PRISM version 5.0 (GraphPad Software Inc., La Jolla, CA, USA), and the IC_{50} value of KR36676 or SB657510 (the concentration required to reduce the radio-isotope [^{125}I] count or the aequorin luminescence count to 50% of the positive control) was calculated. The ID_{50} values of KR36676 or SB657510 (the concentration required to reduce an area under the curve to 50% of the vehicle-treated group) in U-II-induced ear flushing study was calculated. Data were analysed by Student's *t*-test or one-way ANOVA, followed by Dunnett's test for multiple comparisons (Sigma Stat, Jandel Co., San Rafael, CA, USA). In all comparisons, *P*-<0.05 indicated statistical significance.

Materials

Human recombinant U-II and SB657510 (Douglas *et al.*, 2005), a UT receptor antagonist, was purchased from Sigma-Aldrich (St. Louis, MO, USA). KR36676 was synthesized in the Korea Research Institute of Chemical Technology (KRICT, Daejeon, Korea). The aequorin parental cell line (ES-000-A30) was licensed from PerkinElmer Life and Analytical Sciences (Boston, MA, USA). DMEM, FBS and antibiotics were purchased from GIBCO BRL (Grand Island, NY, USA). All other reagents were from Sigma-Aldrich.

Results

Radioligand receptor binding affinity

KR36676 exhibited marked affinity with a K_i value of 0.70 ± 0.05 nM for the UT receptor (Figure 1A), which was lower than that for SB657510 (23.9 ± 7.9 nM) and similar to U-II (0.44 ± 0.07 nM).

Functional antagonism with calcium mobilization

The antagonistic activity of KR36676 was assessed by measuring calcium mobilization in HEK293-aeq/hUT cells. KR36676 inhibited the responses to U-II in a concentration-dependent manner (Figure 1B). The IC_{50} value of KR36676 at 0.1 μM U-II was 4.0 ± 0.4 nM. SB657510, the reference antagonist for the UT receptor, was less potent (IC_{50} value: 18.9 ± 2.3 nM) than KR36676.

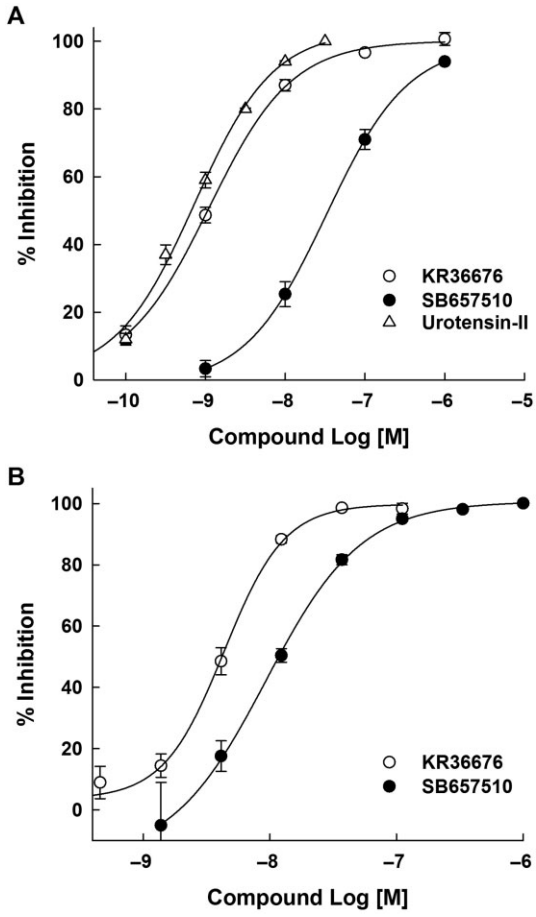

Figure 1

(A) Concentration-response curves of KR36676, U-II and SB657510 for the [^{125}I]-based binding assay for UT receptor. Binding affinity for UT receptors was determined by competitive binding with 0.1 nM [^{125}I] U-II. (B) Antagonist activity of KR36676 and SB657510 for UT receptors. Inhibition of cell-based functional responses by KR36676 and SB657510 were determined by the change of agonist-induced intracellular calcium concentration in HEK293-aeq/hUT cells. Data were expressed as mean ± SEM (n = 3).

Actin stress fibre formation induced by U-II in H9c2$_{UT}$ cells

The actin stress fibre formation assay was performed using rat heart-derived H9c2 cells that overexpressed the hUT receptor. As shown in Figure 2A, treatment with U-II (0.1 μM) alone for 2 h increased the formation of actin stress fibres by approximately 56%, which was significantly inhibited with KR36676 (≥0.003 μM). Suppression of actin stress fibre formation was also observed with SB657510 (0.1 μM).

Cellular hypertrophy induced by U-II in H9c2$_{UT}$ cells

In control H9c2$_{UT}$ cells treated with U-II (0.1 μM) for 24 h, cell size was significantly increased by approximately 46%

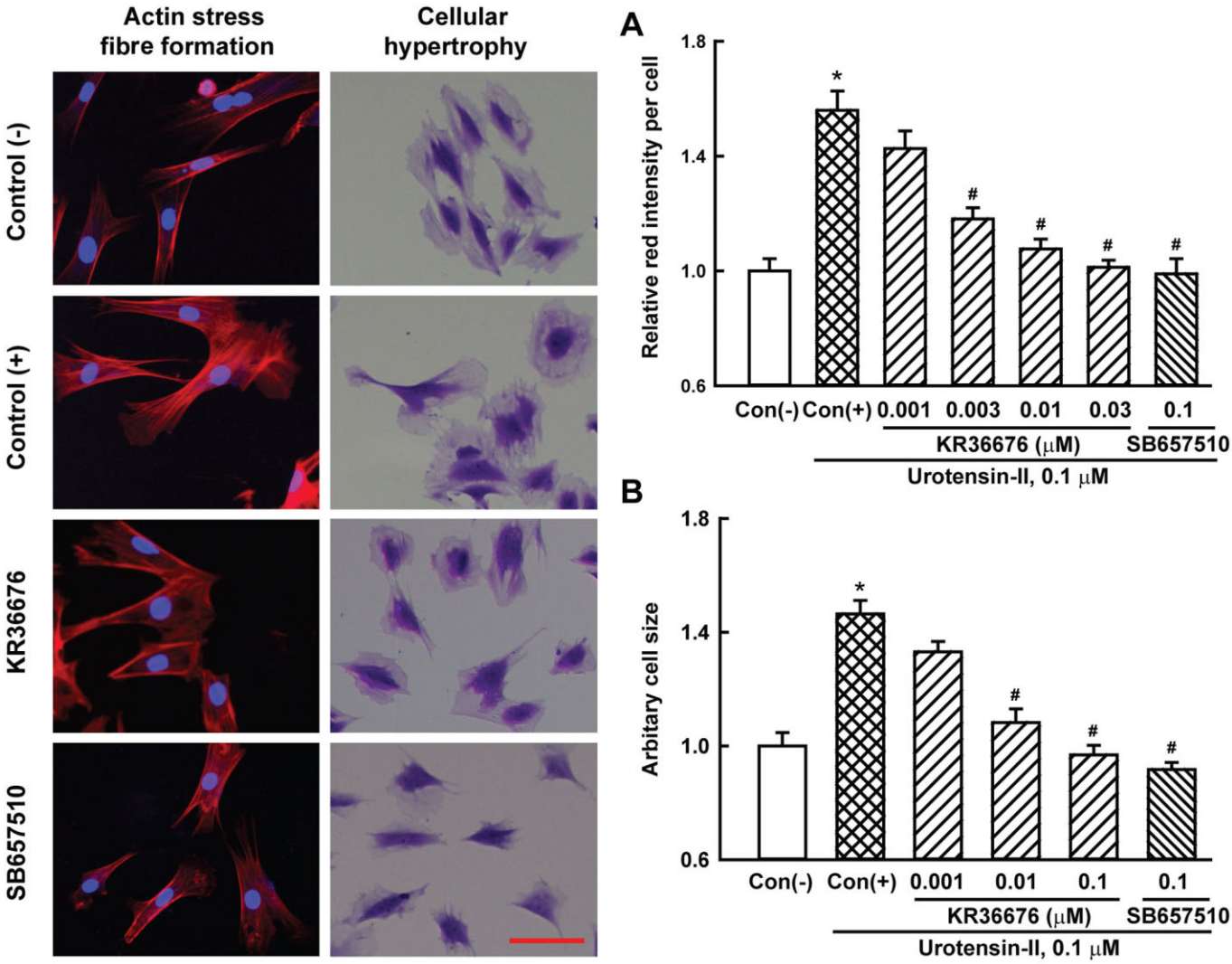

Figure 2

(A) Immunofluorescent staining for actin stress fibre formation in H9c2$_{UT}$ cells. Cells were pretreated with KR36676 and SB657510 at the indicated concentrations for 2 h, and then stimulated with 0.1 μM U-II for 2 h. Actin stress fibre formation was visualized using Alexa Fluor 586 Phalloidin dye. The same fields were counter-stained with Hoeschst 33342 dye to locate the nuclei. The relative red intensities were expressed as mean ± SEM (n = 11–15). (B) Anti-hypertrophic effects of KR36676 and SB657510 in H9c2$_{UT}$ cells. After inducing cellular hypertrophy with 0.1 μM U-II, adherent cells were fixed and stained to obtain images for analysis. Targeted cell size was analysed using Image-Pro PLUS software, and the relative cell sizes were expressed as mean ± SEM (n = 10). Scale bar, 100 μm. *P < 0.05, significantly different from negative control, Con (–): $^{\#}P$ < 0.05, significantly different from positive control, Con (+), stimulated with 0.1 μM U-II.

(Figure 2B), which was significantly inhibited by KR36676 at concentrations below 0.01 μM. Similar inhibitory effects on cellular hypertrophy were also observed with 0.1 μM of SB657510.

Inhibitory effects of KR36676 on U-II-induced ear flushing

Administration of U-II increased ear pinna temperature in conscious rats. As shown in Figure 3, ear pinna temperature (basal temperature: 26.2 ± 0.1°C) was augmented by U-II (10 nmol·kg^{-1}, s.c.) and peaked at 15–21 min (maximum increase: 6.0 ± 0.2°C). Such U-II-induced increases of ear pinna temperature were inhibited by the i.p. injection of KR36676 or SB657510 (ID_{50} values: 1.6 or 5.5 mg·kg^{-1}, respectively) in a dose-dependent manner (Figure 3A and B). The inhibitory effects of KR36676 or SB657510 on U-II-induced ear flushing response were also observed after oral administration (ID_{50} values: 1.6 or 10.3 mg·kg^{-1}, respectively; Figure 3C and D).

Effects of KR36676 on cardiac hypertrophy and ventricular performance after pressure-overload in mice

In order to study the anti-hypertrophic effect of KR36676 in pathological cardiac remodelling conditions, we used the pressure-overload cardiac hypertrophy model induced

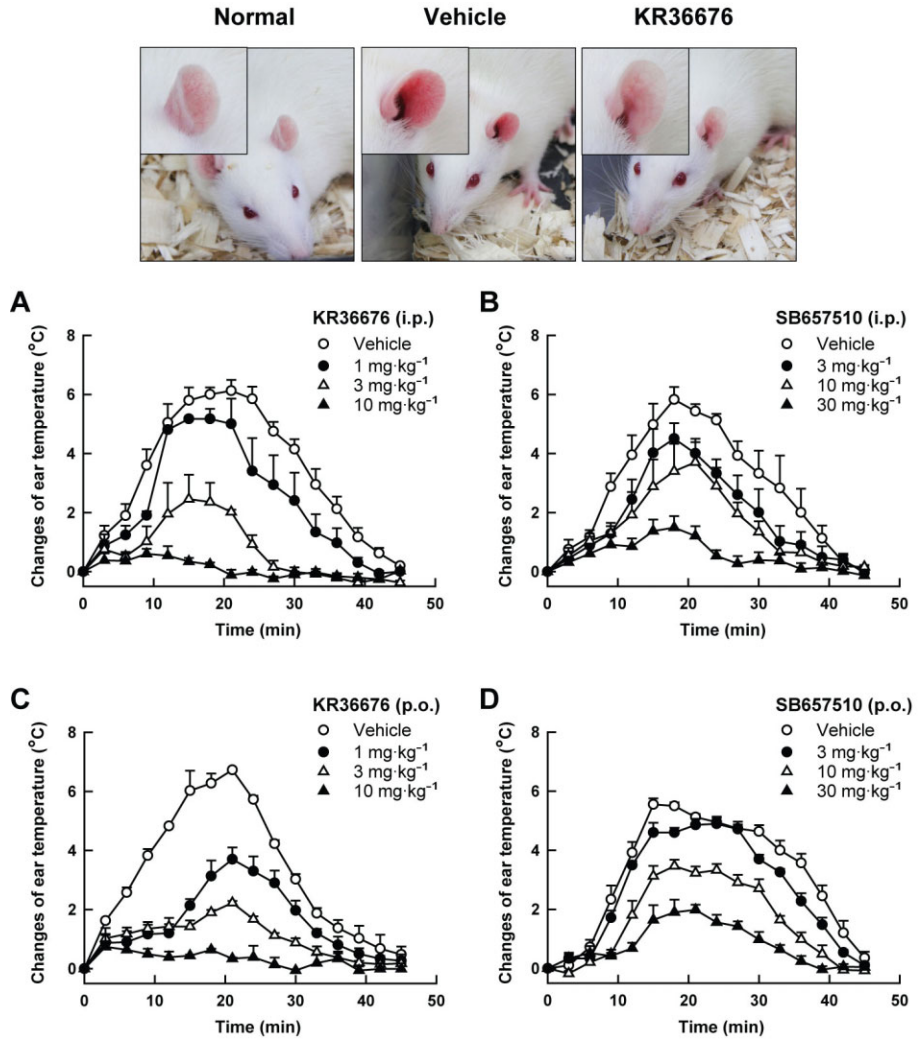

Figure 3

The inhibitory effects of KR36676 and SB657510 on U-II-induced increase in ear pinna surface temperature. Five minutes prior to U-II (10 nmol·kg^{-1}; s.c.) injection, KR36676 (A), SB657510 (B) or vehicle (polyethylene glycol 400) were given i.p.. For oral administration, KR36676 (C), SB657510 (D) or vehicle (0.5% carboxymethyl cellulose) was given 30 min before the U-II injection. Changes of ear temperature are expressed as mean ± SEM (n = 4–5).

by TAC in wild-type C57BL/6 mice. Two weeks post-operatively, the vehicle-treated group exhibited a markedly higher ratio of LVW/TL (mg·mm^{-1}; Figure 4A) and HW/TL (Figure 4B) compared with the sham-operated group. Consistent with the *in vitro* results, oral administration of KR36676 (10 or 30 mg·kg^{-1}) decreased the development of cardiac hypertrophy (43.1 and 62.3% for % decrease in LVW, respectively, $P < 0.05$, Figure 4). This anti-hypertrophic effect was comparable with that in the captopril-treated group.

Histological analysis demonstrated that TAC caused a significant increase in myocyte cross-sectional area (Figure 5A) compared with the sham-operated group. The TAC-induced increases in myocyte hypertrophy were significantly inhibited with KR36676. In the mechanisms study involving cardiac hypertrophy, the phosphorylation of p38 and ERK1/2 were notably higher in the TAC group compared with the sham group (Figure 5B and C). However, TAC did not induce activation of JNK (Figure 5D). The increased phosphorylation of ERK1/2 was attenuated by KR36676 (30 mg·kg^{-1}; Figure 5B), but phosphorylation of p38 was not decreased (Figure 5C). The TAC-induced fibrosis was observed both in interstitial (Figure 6A) and perivascular regions (Figure 6B) and was decreased by KR36676 (Figure 6). At 2 weeks after TAC, the vehicle-treated group showed significantly higher LVSP and +dP/dt$_{max}$ than the sham-operated group and these haemodynamic changes were prevented by KR36676 (30 mg·kg^{-1}) (Table 1).

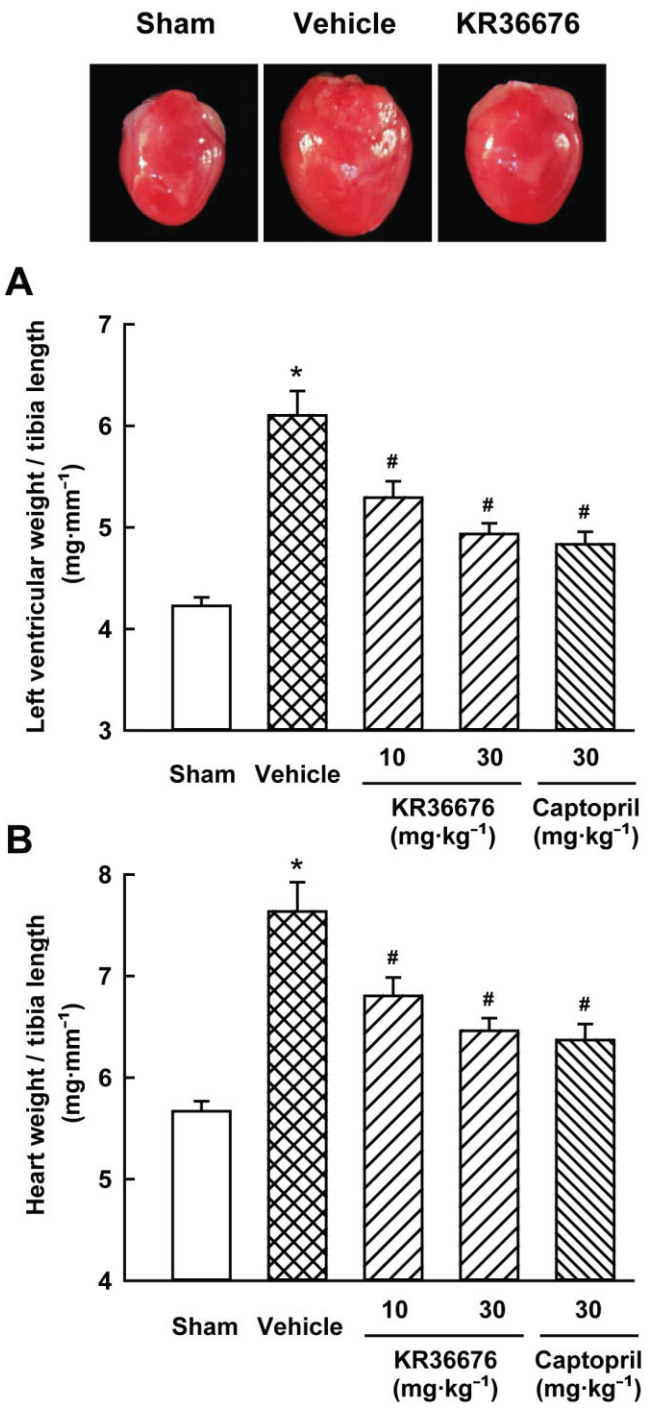

Figure 4

Effects of KR36676 on cardiac hypertrophy in TAC-induced cardiac hypertrophy in mice. (A) LV weight to tibia length ratio and (B) heart weight to tibia length ratio was determined 2 weeks after TAC or sham surgery. Values are mean percentage ± SEM (n = 17–18). *P < 0.05, significantly different from the sham-operated group; #P < 0.05, significantly different from the vehicle-treated group.

Effects of KR36676 on cardiac hypertrophy and function after MI in rats

Anti-hypertrophic effect of KR36676 was confirmed in another animal model, cardiac remodelling following MI in rats. Although there are no differences in LV mass between the groups, myocyte cross-sectional area was significantly increased compared with the sham group at 4 weeks after MI (Figure 7). This MI-induced cardiomyocyte hypertrophy was significantly reduced by KR36676 (30 mg·kg^{-1}). Although the infarct size was not different between each group, the infarct expansion index was lower after KR36676 treatment (Table 2). Haemodynamic data are summarized in Table 2. At 4 weeks after MI, the vehicle-treated group had worse ejection fraction, cardiac output and stroke volume than the sham group and KR36676 preserved cardiac function (Table 2). Although only little or weak immunoreactivity for U-II and UT receptors (brown colour) was observed in heart tissue from the sham group, the immunoreactivity for these markers was much stronger in the peri-infarct zone both of vehicle and KR36676-treated group (Figure 7).

Receptor selectivity profiling

As shown in Table 3, 1 μM KR36676 showed in appreciable interactions (>90% inhibition) with opioid κ, μ receptors. In addition, KR36676 also showed lower affinities (60–80% inhibition) for other receptors including the site 2 sodium channel, dopamine and noradrenaline transporters. Other than those targets, less than 50% inhibition was seen at 1 or 10 μM KR36676.

Pharmacokinetic study

The primary pharmacokinetic parameters and plasma profiles for KR36676 are summarized (see Supporting Information Table S1). The AUC_{∞} were 0.9 ± 0.1 and 0.4 ± 0.2 μg·h·mL^{-1} after i.v. injection and oral administration at 10 mg·kg^{-1} respectively, demonstrating almost 50% bioavailability. The $t_{1/2}$ values were 5.7 ± 0.7 and 42.1 ± 24.2 h after i.v. injection and oral administration respectively. In tissue distribution studies, the concentration of KR36676 in whole blood was three times higher than that in plasma. Moreover, the concentrations of KR36676 in liver, heart and kidney was 55, 48 and 88 times higher respectively (see Supporting Information Table S2).

Discussion and conclusions

In this study, we have presented data to show that an orally active UT receptor antagonist, KR36676, exerted anti-hypertrophic effects in the heart both *in vitro* and *in vivo*.

Recently, we have identified KR36676 as a novel UT receptor antagonist. The receptor binding results indicated that KR36676 had marked affinity for the UT receptor (K_i value: 0.70 nM), which is similar to U-II (0.44 nM). Furthermore, KR36676 possessed 5- to 1000-fold greater UT receptor binding activity than for 86 other distinct mammalian GPCRs, ion channels and neurotransmitter uptake targets. In terms of functional antagonism, KR36676 inhibited the U-II-evoked calcium mobilization with an IC_{50} value of 4.0 nM, which was more potent than that of SB657510 (IC_{50} value: 18.9 nM). This

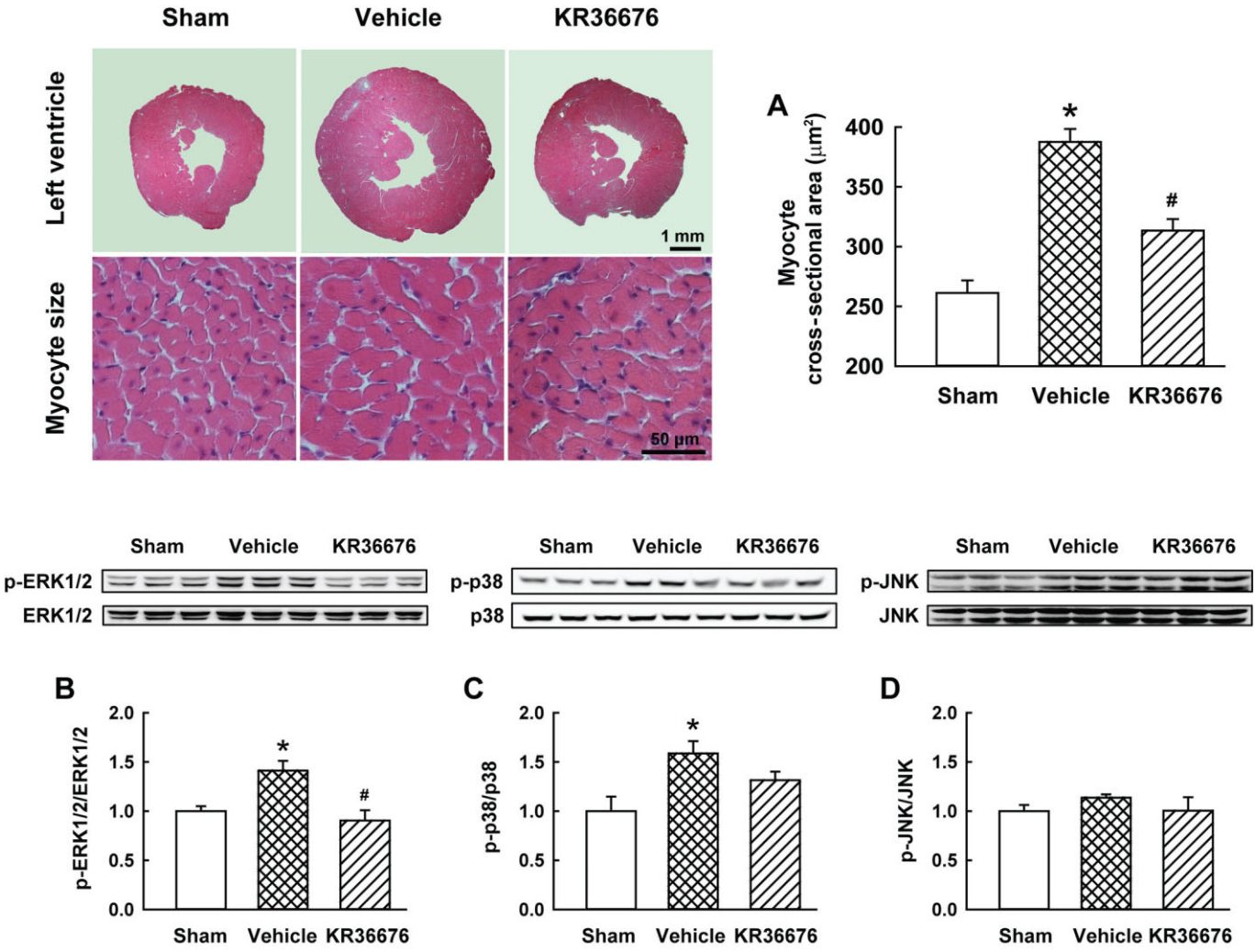

Figure 5

Effects of KR36676 (30 mg·kg^{-1}) on myocyte hypertrophy and MAPK activation in TAC-induced cardiac hypertrophy in mice. Left upper photographs: representative examples of sections stained with haematoxylin and eosin (H&E) in LV wall of each group. (A) Cardiomyocyte cross-sectional area (μm^2) ($n = 17$) and (B–D) comparison of MAPK activation ($n = 3$–4) were determined 2 weeks after TAC or sham surgery. Values are mean percentage ± SEM. *$P < 0.05$, significantly different from the sham-operated group: $^{\#}P < 0.05$, significantly different from the vehicle-treated group.

in vitro functional assay based on the calcium-sensitive photoprotein, aequorin, is well established as an efficient system for the characterization of GPCRs (Le Poul *et al.*, 2002; Gilchrist *et al.*, 2008).

Inappropriate regulation of actin stress fibre formation is directly involved in numerous pathological situations including cardiovascular diseases and cancer (Chaponnier and Gabbiani, 2004). Although the mechanism responsible for the regulation of stress fibre formation remains to be elucidated, the pro-fibrogenic effects of U-II are well known and U-II can induce actin stress fibre formation and arterial smooth muscle contraction through the activation of the small GTPase RhoA and its downstream effector Rho-kinase (Sauzeau *et al.*, 2001; Matsusaka and Wakabayashi, 2006). In our study, KR36676 markedly suppressed the formation of actin stress fibres induced by U-II in H9c2$_{UT}$ cells, suggesting that KR36676 blocked the pathophysiological actions of U-II related to inappropriate actin stress fibre formation, through its antagonism of UT receptor.

Increasing evidence has suggested that U-II may be an important determinant of cardiac hypertrophy in conditions characterized by UT receptor up-regulation (Tzanidis *et al.*, 2003; Zhang *et al.*, 2007). In the cellular hypertrophy study with H9c2$_{UT}$ cells, U-II increased H9c2$_{UT}$ cell size by 46%. This cellular change was inhibited by KR36676 in a concentration-dependent manner, suggesting that KR36676 has potent anti-hypertrophic effects in H9c2$_{UT}$ cells by targeting the UT receptor.

Next, we examined whether KR36676 is able to block U-II-mediated physiological effects *in vivo*. First, the acute response to KR36676 was evaluated in a U-II-induced ear flushing model. Recently, it has been reported that U-II

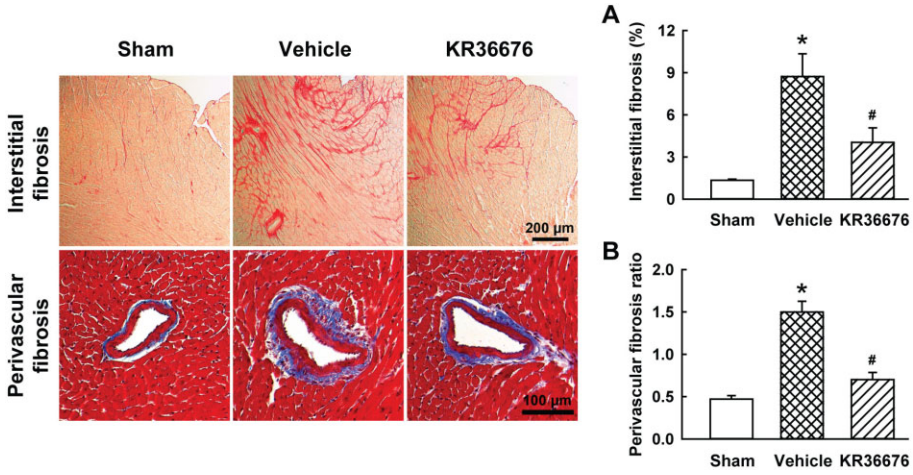

Figure 6

Effects of KR36676 (30 mg·kg^{-1}) on myocardial fibrosis in TAC-induced cardiac hypertrophy in mice. Micrographs are representative of sections stained with Picrosirius Red and Masson's trichrome in LV wall of each group. (A) Interstitial fibrosis (%) and (B) perivascular fibrosis ratio were determined 2 weeks after TAC or sham surgery. Values are mean percentage ± SEM (n = 17). *P < 0.05, significantly different from the sham-operated group; $^{\#}P$ < 0.05, significantly different from the vehicle-treated group.

Table 1

Morphometric and haemodynamic parameters 2 weeks after TAC or sham surgery

			KR36676		Captopril
	Sham	Vehicle	10 mg·kg^{-1}	30 mg·kg^{-1}	30 mg·kg^{-1}
n	17	18	17	17	17
Body weight (g)	23.7 ± 0.4	22.9 ± 0.4	23.5 ± 22.8	22.8 ± 0.3	23.4 ± 0.3
Heart weight (mg)	96.3 ± 1.7	127.8 ± 5.1*	115.1 ± 3.1$^{\#}$	108.6 ± 2.4$^{\#}$	108.1 ± 2.9$^{\#}$
Ventricular weight (mg)	92.1 ± 1.7	122.3 ± 4.9*	110.1 ± 3.0$^{\#}$	103.6 ± 2.5$^{\#}$	103.0 ± 2.6$^{\#}$
Atrial weight (mg)	4.2 ± 0.5	5.5 ± 0.5	4.9 ± 0.3	5.0 ± 0.3	5.1 ± 0.4
Lung weight (mg)	114.2 ± 1.4	117.9 ± 5.5	114.2 ± 2.7	113.8 ± 1.8	113.6 ± 4.8
n	10	6	7	7	6
HR (beats per min)	371.4 ± 13.9	398.5 ± 37.8	365.9 ± 17.6	361.0 ± 8.4	413.2 ± 13.5
LVSP (mmHg)	105.4 ± 4.1	180.0 ± 4.7*	149.7 ± 4.5$^{\#}$	141.9 ± 6.1$^{\#}$	137.8 ± 10.9$^{\#}$
LVEDP (mmHg)	6.2 ± 2.9	6.5 ± 4.3	6.7 ± 4.8	6.6 ± 3.1	6.2 ± 2.8
LV +dP/dt$_{max}$ (mmHg·s^{-1})	6484 ± 234	8315 ± 275*	6442 ± 255$^{\#}$	6732 ± 203$^{\#}$	6861 ± 636$^{\#}$
LV –dP/dt$_{max}$ (mmHg·s^{-1})	–6255 ± 172	–8305 ± 313*	–7202 ± 330	–7439 ± 441	–6301 ± 539$^{\#}$

HR, heart rate; LV dP/dt$_{max}$, positive (+dP/dt) and negative (–dP/dt) maximum rate of pressure in left ventricle; LVSP, left ventricular systolic pressure. Data were expressed as mean ± SEM. *P < 0.05, significantly different from the sham group. $^{\#}P$ < 0.05, significantly different from the vehicle-treated group.

induces ear flushing in conscious rats by specifically activating peripheral UT receptors, an effect that can be readily quantified by serial measurements of ear surface temperature (Qi *et al.*, 2007). From this acute and reproducible experimental model, *in vivo* efficacy of UT receptor antagonists can be easily estimated before applying to long-term heart failure studies on animals (Luci *et al.*, 2007; Qi *et al.*, 2007; Lawson *et al.*, 2009). In the ear flushing study, oral administration of KR36676 clearly prevented U-II-induced elevation of surface temperature on the ear pinna in a dose-dependent manner. Together with pharmacokinetic data, our results strongly suggest that KR36676 could be an orally effective and potent

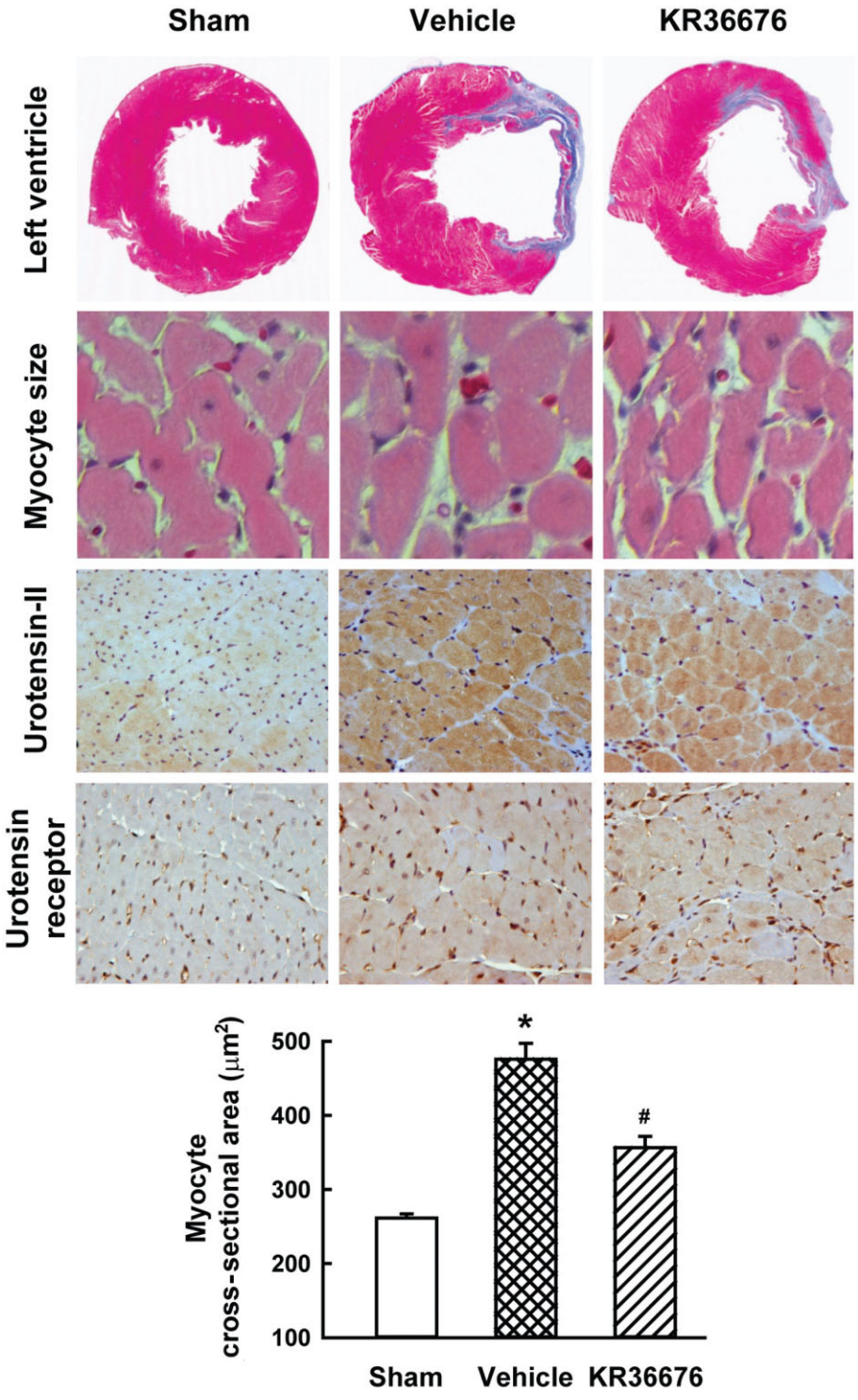

Figure 7

Effects of KR36676 (30 mg·kg^{-1}) on cardiac hypertrophy and cardiac function in rats with MI-induced cardiac hypertrophy. Representative examples of sections stained with Masson's trichrome, haematoxylin and eosin, and immunoreactivity of U-II and UT receptor in the peri-infarct zone of each group. Cardiomyocyte cross-sectional area (μm^2) was determined 4 weeks after MI. Values are mean percentage ± SEM (n = 15–16). *P < 0.05, significantly different from the sham-operated group and $^{\#}P$ < 0.05, significantly different from the vehicle-treated group.

Table 2

Morphometric and haemodynamic parameters 4 weeks after LAD ligation or sham surgery

	Sham	Vehicle	KR36676 (30 mg·kg^{-1})
n	15	16	15
BW (before, g)	273.1 ± 4.5	265.4 ± 3.9	268.3 ± 4.5
BW (after, g)	435.6 ± 8.5	408.2 ± 7.3	392.3 ± 6.1
RA/BW (mg·g^{-1})	0.068 ± 0.003	0.085 ± 0.006	0.082 ± 0.005
LA/BW (mg·g^{-1})	0.071 ± 0.003	0.076 ± 0.003	0.071 ± 0.004
RV/BW (mg·g^{-1})	0.491 ± 0.011	0.507 ± 0.012	0.528 ± 0.012
(LV+S)/BW (mg·g^{-1})	1.792 ± 0.031	1.992 ± 0.041	2.010 ± 0.046
Lung/BW (mg·g^{-1})	2.638 ± 0.053	2.725 ± 0.046	2.724 ± 0.063
Infarct size (%)	0 ± 0	27.9 ± 4.3	21.3 ± 4.3
Expansion index	0 ± 0	0.778 ± 0.118	0.471 ± 0.087$^{\#}$
HR (beats·per min)	416.1 ± 7.2	422.2 ± 7.8	447.7 ± 8.4
LVSP (mmHg)	133.9 ± 1.9	130.1 ± 2.9	145.0 ± 3.7
LVEDP (mmHg)	7.4 ± 0.6	7.8 ± 0.6	7.3 ± 0.4
SV (μL)	104.8 ± 5.1	79.8 ± 8.2	91.1 ± 10.0
CO (mL·min^{-1})	43.5 ± 2.1	33.7 ± 3.5	41.0 ± 4.7
EF (%)	59.3 ± 4.2	36.5 ± 3.7*	43.2 ± 6.0
SW (mmHg·mL)	9.7 ± 0.5	6.9 ± 0.8*	8.3 ± 0.8
+dP/dt$_{max}$ (mmHg·s^{-1})	9539.8 ± 284.4	8706.3 ± 333.7	10 154.6 ± 5 559.4$^{\#}$
–dP/dt$_{max}$ (mmHg·s^{-1})	–11 406.7 ± 539.3	–9001.4 ± 502.9*	–11 197.7 ± 717.7$^{\#}$

BW, body weight; CO, cardiac output; EF, ejection fraction; HR, heart rate; LA, left atrium; LV dP/dt$_{max}$, positive (+dP/dt) and negative (–dP/dt) maximum rate of pressure in left ventricle; LV+S, left ventricle plus septum; LVEDP, left ventricular end-diastolic pressure; LVSP, left ventricular systolic pressure; RA, right atrium; RV, right ventricle; SV, stroke volume; SW, stroke work. Data were expressed as mean ± SEM. *P < 0.05, significantly different from the sham group. $^{\#}P$ < 0.05, significantly different from the vehicle-treated group.

UT receptor antagonist that can delineate the physiological actions of U-II *in vivo*.

Finally, we evaluated the effects of KR36676 in two animal models of cardiac hypertrophy. Consistent with the *in vitro* results of cellular hypertrophy, oral administration of KR36676 (10 or 30 mg·kg^{-1}) significantly reduced the development of LV hypertrophy and cardiac fibrosis induced by TAC. The activation of MAPK has been shown to play an important role in the development of cardiac hypertrophy induced by TAC (Heineke and Molkentin, 2006) and U-II increases cardiomyocyte hypertrophy via MAPK (Onan *et al.*, 2004). In the TAC study after 2 weeks, ERK1/2 and p38 have been reported to significantly contribute to the induction of cardiac hypertrophy (Si *et al.*, 2014). When KR36676 was used in our TAC model, the TAC-induced phosphorylation of ERK1/2 was markedly reduced, suggesting that the anti-hypertrophic effects of KR36676 via antagonism of UT receptors also involved inhibition of ERK1/2 phosphorylation. Furthermore, administration of KR36676 (30 mg·kg^{-1}) prevented the cardiomyocyte enlargement and ameliorated cardiac dysfunction in MI-induced cardiac remodelling in rats. In an earlier report, the critical role of U-II and the UT receptor in the development of cardiac hypertrophy has been described (Papadopoulos *et al.*, 2008). However, there are only a few studies reporting the positive effects of UT receptor antagonists in an animal model of ventricular hypertrophy. Here, our results introduce, for the first time, a novel non-peptide UT receptor antagonist possessing potent anti-hypertrophic effects both in infarcted and pressure-overloaded rodent hearts. In this study, some characteristic pathophysiological features of heart failure were not assessed because our experiments were conducted during the relatively early stages of both the TAC and MI models. Therefore, further studies are needed to evaluate cardio-protective effects of KR36676 in long-term heart failure animal models.

In summary, the present studies demonstrated that KR36676 is a UT receptor antagonist having both a high affinity and potency for the receptor. In the rat heart-derived H9c2$_{UT}$ cell, KR36676 blocked U-II-induced stress fibre formation and cellular hypertrophy. Notably, the oral administration of KR36676 in animal models of pressure overload and MI significantly reduced LV hypertrophy and cardiac dysfunction with a good oral bioavailability. Based on these findings, we suggest that KR36676 could be developed as an effective UT receptor antagonist for clinical application and that this compound will also be a useful tool for defining the role of UT receptors in the field of cardiac hypertrophy.

Table 3

Receptor selectivity profiling for KR36676

Target	Species	Concentration of KR36676	% inhibition	Target	Species	Concentration of KR36676	% inhibition
ATPase, Na^+/K^+, heart	Pig	10 μM	0	Adrenoceptor α_{1A}	Rat	1 μM	21
Cholinesterase, acetyl, ACES	Human	10 μM	16	Adrenoceptor α_{1B}	Rat	1 μM	24
COX-1	Human	10 μM	20	Adrenoceptor α_{2A}	Human	1 μM	32
COX-2	Human	10 μM	0	Adrenoceptor α_{2B}	Human	1 μM	30
Monoamine oxidase MAO-A	Human	10 μM	24	Adrenoceptor β_1	Human	1 μM	5
Monoamine oxidase MAO-B	Human	10 μM	1	Androgen (testosterone)	Human	1 μM	2
Peptidase, ACE	Rabbit	10 μM	0	Angiotensin AT_1	Human	1 μM	7
Peptidase, CTSG (cathepsin G)	Human	10 μM	0	Calcium channel L-type, phenylalkylamine	Rat	1 μM	47
PDE3	Human	10 μM	8	Cannabinoid CB_1	Human	1 μM	16
PDE4	Human	10 μM	21	Cholecystokinin CCK_1	Human	1 μM	18
Protein serine/threonine kinase, PKC, non-selective	Rat	10 μM	31	Dopamine D_1	Human	1 μM	9
Protein tyrosine kinase, insulin receptor	Human	10 μM	6	Dopamine D_{2L}	Human	1 μM	19
Protein tyrosine kinase, LCK	Human	10 μM	0	Dopamine D_{2S}	Human	1 μM	25
Adenosine A_1	Human	10 μM	0	Histamine H_1	Human	1 μM	13
Adenosine A_{2A}	Human	10 μM	0	Histamine H_2	Human	1 μM	54
Adrenoceptor α_{1D}	Human	10 μM	32	Melanocortin MC_4	Human	1 μM	9
Adrenoceptor β_2	Human	10 μM	11	Muscarinic M_1	Human	1 μM	2
Bradykinin B_2	Human	10 μM	0	Neuropeptide YY_1	Human	1 μM	12
Calcium channel L-type, benzothiazepine	Rat	10 μM	39	Opioid δ_1	Human	1 μM	28
Calcium channel L-type, dihydropyridine	Rat	10 μM	32	Opioid κ	Human	1 μM	**100**
Calcium channel N-type	Rat	10 μM	9	Opioid μ	Human	1 μM	**98**
Cannabinoid CB_2	Human	10 μM	25	Progesterone PR-B	Human	1 μM	29
Chemokine CCR1	Human	10 μM	0	5-HT_{1A} receptor	Human	1 μM	49
Chemokine CCR2	Human	10 μM	17	5-HT_{1B} receptor	Human	1 μM	17
Cholecystokinin CCK_2	Human	10 μM	5	5-HT_{2A} receptor	Human	1 μM	53

Endothelin ET_A	Human	10 μM	28	$5\text{-}HT_{2B}$ receptor	Human	1 μM	36
Oestrogen ERα	Human	10 μM	24	$5\text{-}HT_{2C}$ receptor	Human	1 μM	45
$GABA_A$, chloride channel, TBOB	Rat	10 μM	6	Sodium channel, site 2	Rat	1 μM	**82**
$GABA_A$, flunitrazepam, central	Rat	10 μM	9	Tachykinin NK_1	Human	1 μM	9
$GABA_A$, Ro-15–1788, hippocampus	Rat	10 μM	2	Transporter, dopamine (DAT)	Human	1 μM	**68**
$GABA_{B1A}$	Human	10 μM	32	Transporter, GABA	Rat	1 μM	0
Glucocorticoid	Human	10 μM	29	Transporter, noradrenaline (NET)	Human	1 μM	**62**
Glutamate, AMPA	Rat	10 μM	11	Transporter, 5-HT (SERT)	Human	1 μM	39
Glutamate, kainate	Rat	10 μM	1				
Glutamate, metabotropic, $mGlu_5$	Human	10 μM	3				
Glutamate, NMDA, agonism	Rat	10 μM	13				
Glutamate, NMDA, glycine	Rat	10 μM	14				
Glutamate, NMDA, phencyclidine	Rat	10 μM	5				
Glutamate, NMDA, polyamine	Rat	10 μM	3				
Glycine, strychnine-sensitive	Rat	10 μM	38				
LT, cysteinyl $CysLT_1$	Human	10 μM	13				
Melanocortin MC_1	Human	10 μM	41				
Muscarinic M_2	Human	10 μM	34				
Muscarinic M_3	Human	10 μM	45				
Muscarinic M_4	Human	10 μM	36				
Nicotinic ACh	Human	10 μM	7				
Nicotinic ACh α1, bungarotoxin	Human	10 μM	17				
Platelet activating factor (PAF)	Human	10 μM	16				
Potassium channel (K_{ATP})	Human	10 μM	0				
PPARγ	Human	10 μM	7				
$5\text{-}HT_3$ receptor	Human	10 μM	29				
Transporter, adenosine	Guinea pig	10 μM	11				
Vasopressin V_{1A}	Human	10 μM	16				

The final concentration of KR36676 used in the assay was kept at 1 or 10 μM and the results were expressed as % inhibition relative to the control reaction without an antagonist. Results with more than 60% of inhibition are bold typeface.

Acknowledgements

This study was supported by the Bio & Medical Technology Development Program of the National Research Foundation funded by the Korean government (2011–0019397).

Author contributions

B. H. L. conceived the study; K. S. O., J. H. L., C. H. P., H. W. S. , K. Y. Y., C. J. L. and S. L. performed the experiments; K. S. O., J. H. L. and B. H. L. analysed the data; K. S. O., J. H. L., S. L. and B. H. L. prepared the manuscript.

Conflict of interest

The authors state no conflict of interest.

References

Alexander SPH, Benson HE, Faccenda E, Pawson AJ, Sharman JL, Spedding M *et al*. (2013a). The Concise Guide to PHARMACOLOGY 2013/14: G Protein-Coupled Receptors. Br J Pharmacol 170: 1459–1581.

Alexander SPH, Benson HE, Faccenda E, Pawson AJ, Sharman JL, Spedding M *et al*. (2013b). The Concise Guide to PHARMACOLOGY 2013/14: Enzymes. Br J Pharmacol, 170: 1797–1867.

Alhaddad IA, Tkaczevski L, Siddiqui F, Mir R, Brown EJ Jr (1995). Aspirin enhances the benefits of late reperfusion on infarct shape. A possible mechanism of the beneficial effects of aspirin on survival after acute myocardial infarction. Circulation 91: 2819–2823.

Ames RS, Sarau HM, Chambers JK, Willette RN, Aiyar NV, Romanic AM *et al*. (1999). Human urotensin-II is a potent vasoconstrictor and agonist for the orphan receptor GPR14. Nature 401: 282–286.

Barrette PO, Schwertani AG (2012). A closer look at the role of urotensin II in the metabolic syndrome. Front Endocrinol (Lausanne) 3: 165.

Bousette N, Giaid A (2006). Urotensin-II and cardiovascular diseases. Curr Hypertens Rep 8: 479–483.

Bousette N, Hu F, Ohlstein EH, Dhanak D, Douglas SA, Giaid A (2006). Urotensin-II blockade with SB-611812 attenuates cardiac dysfunction in a rat model of coronary artery ligation. J Mol Cell Cardiol 41: 285–295.

Chaponnier C, Gabbiani G (2004). Pathological situations characterized by altered actin isoform expression. J Pathol 204: 386–395.

deAlmeida AC, van Oort RJ, Wehrens XH (2010). Transverse aortic constriction in mice. J Vis Exp 38: 1729.

Douglas SA, Ohlstein EH (2000). Human urotensin-II, the most potent mammalian vasoconstrictor identified to date, as a therapeutic target for the management of cardiovascular disease. Trends Cardiovasc Med 10: 229–237.

Douglas SA, Behm DJ, Aiyar NV, Naselsky D, Disa J, Brooks DP *et al*. (2005). Nonpeptidic urotensin-II receptor antagonists I: in vitro pharmacological characterization of SB-706375. Br J Pharmacol 145: 620–635.

Esposito G, Perrino C, Cannavo A, Schiattarella GG, Borgia F, Sannino A *et al*. (2011). EGFR trans-activation by urotensin II receptor is mediated by beta-arrestin recruitment and confers cardioprotection in pressure overload-induced cardiac hypertrophy. Basic Res Cardiol 106: 577–589.

Fishbein MC, Maclean D, Maroko PR (1978). Experimental myocardial infarction in the rat: qualitative and quantitative changes during pathologic evolution. Am J Pathol 90: 57–70.

Gilchrist MA 2nd, Cacace A, Harden DG (2008). Characterization of the 5-HT2b receptor in evaluation of aequorin detection of calcium mobilization for miniaturized GPCR high-throughput screening. J Biomol Screen 13: 486–493.

Gruson D, Ginion A, Decroly N, Lause P, Vanoverschelde JL, Ketelslegers JM *et al*. (2010). Urotensin II induction of adult cardiomyocytes hypertrophy involves the Akt/GSK-3beta signaling pathway. Peptides 31: 1326–1333.

Heineke J, Molkentin JD (2006). Regulation of cardiac hypertrophy by intracellular signalling pathways. Nat Rev Mol Cell Biol 7: 589–600.

Johns DG, Ao Z, Naselsky D, Herold CL, Maniscalco K, Sarov-Blat L *et al*. (2004). Urotensin-II-mediated cardiomyocyte hypertrophy: effect of receptor antagonism and role of inflammatory mediators. Naunyn Schmiedebergs Arch Pharmacol 370: 238–250.

Kilkenny C, Browne W, Cuthill IC, Emerson M, Altman DG (2010). Animal research: Reporting *in vivo* experiments: the ARRIVE guidelines. Br J Pharmacol 160: 1577–1579.

Kompa AR, Wang BH, Phrommintikul A, Ho PY, Kelly DJ, Behm DJ *et al*. (2010). Chronic urotensin II receptor antagonist treatment does not alter hypertrophy or fibrosis in a rat model of pressure-overload hypertrophy. Peptides 31: 1523–1530.

Lawson EC, Luci DK, Ghosh S, Kinney WA, Reynolds CH, Qi J *et al*. (2009). Nonpeptide urotensin-II receptor antagonists: a new ligand class based on piperazino-phthalimide and piperazino-isoindolinone subunits. J Med Chem 52: 7432–7445.

Le Poul E, Hisada S, Mizuguchi Y, Dupriez VJ, Burgeon E, Detheux M (2002). Adaptation of aequorin functional assay to high throughput screening. J Biomol Screen 7: 57–65.

Li Y, Zhao S, Wang Y, Chen Y, Lin Y, Zhu N *et al*. (2014). Urotensin II promotes atherosclerosis in cholesterol-fed rabbits. PLoS ONE 9: e95089.

Liu JC, Chen CH, Chen JJ, Cheng TH (2009). Urotensin II induces rat cardiomyocyte hypertrophy via the transient oxidization of Src homology 2-containing tyrosine phosphatase and transactivation of epidermal growth factor receptor. Mol Pharmacol 76: 1186–1195.

Luci DK, Ghosh S, Smith CE, Qi J, Wang Y, Haertlein B *et al*. (2007). Phenylpiperidine-benzoxazinones as urotensin-II receptor antagonists: synthesis, SAR, and in vivo assessment. Bioorg Med Chem Lett 17: 6489–6492.

Matsusaka S, Wakabayashi I (2006). Enhancement of vascular smooth muscle cell migration by urotensin II. Naunyn Schmiedebergs Arch Pharmacol 373: 381–386.

McGrath J, Drummond G, McLachlan E, Kilkenny C, Wainwright C (2010). Guidelines for reporting experiments involving animals: the ARRIVE guidelines. Br J Pharmacol 160: 1573–1576.

McKinsey TA, Olson EN (2005). Toward transcriptional therapies for the failing heart: chemical screens to modulate genes. J Clin Invest 115: 538–546.

Oh KS, Lee S, Yi KY, Seo HW, Koo HN, Lee BH (2009). A novel and orally active poly(ADP-ribose) polymerase inhibitor, KR-33889

[2-[methoxycarbonyl(4-methoxyphenyl) methylsulfanyl]-1H-benzimidazole-4-carboxylic acid amide], attenuates injury in in vitro model of cell death and in vivo model of cardiac ischemia. J Pharmacol Exp Ther 328: 10–18.

Onan D, Pipolo L, Yang E, Hannan RD, Thomas WG (2004). Urotensin II promotes hypertrophy of cardiac myocytes via mitogen-activated protein kinases. Mol Endocrinol 18: 2344–2354.

Papadopoulos P, Bousette N, Giaid A (2008). Urotensin-II and cardiovascular remodeling. Peptides 29: 764–769.

Pawson AJ, Sharman JL, Benson HE, Faccenda E, Alexander SP, Buneman OP *et al.*; NC-IUPHAR (2014). The IUPHAR/BPS Guide to PHARMACOLOGY: an expert-driven knowledge base of drug targets and their ligands. Nucl. Acids Res. 42 (Database Issue): D1098–1106.

Qi JS, Schulingkamp R, Parry TJ, Colburn R, Stone D, Haertlein B *et al.* (2007). Urotensin-II induces ear flushing in rats. Br J Pharmacol 150: 415–423.

Ross B, McKendy K, Giaid A (2010). Role of urotensin II in health and disease. Am J Physiol Regul Integr Comp Physiol 298: R1156–R1172.

Sauzeau V, Le Mellionnec E, Bertoglio J, Scalbert E, Pacaud P, Loirand G (2001). Human urotensin II-induced contraction and arterial smooth muscle cell proliferation are mediated by RhoA and Rho-kinase. Circ Res 88: 1102–1104.

Si L, Xu J, Yi C, Xu X, Wang F, Gu W *et al.* (2014). Asiatic acid attenuates cardiac hypertrophy by blocking transforming growth factor-beta1-mediated hypertrophic signaling in vitro and in vivo. Int J Mol Med 34: 499–506.

Tsoukas P, Kane E, Giaid A (2011). Potential clinical implications of the urotensin II receptor antagonists. Front Pharmacol 2: 38.

Tzanidis A, Hannan RD, Thomas WG, Onan D, Autelitano DJ, See F *et al.* (2003). Direct actions of urotensin II on the heart: implications for cardiac fibrosis and hypertrophy. Circ Res 93: 246–253.

You Z, Genest J Jr, Barrette PO, Hafiane A, Behm DJ, D'Orleans-Juste P *et al.* (2012). Genetic and pharmacological manipulation of urotensin II ameliorate the metabolic and atherosclerosis sequalae in mice. Arterioscler Thromb Vasc Biol 32: 1809–1816.

Zhang YG, Li YG, Liu BG, Wei RH, Wang DM, Tan XR *et al.* (2007). Urotensin II accelerates cardiac fibrosis and hypertrophy of rats induced by isoproterenol. Acta Pharmacol Sin 28: 36–43.

Supporting information

Additional Supporting Information may be found in the online version of this article at the publisher's web-site:

http://dx.doi.org/10.1111/bph.13082

Table S1 Pharmacokinetic parameters of KR36676, given i.v or orally to male Sprague-Dawley rats.
Table S2 Tissue distribution of KR36676 in male Sprague-Dawley rats.